Nature of environmentally assisted fracture nucleation and crack growth in polycrystals

Leonardo Golubović, Anatoli Peredera, and Mirjana Golubović

Physics Department, West Virginia University, Morgantown, West Virginia 26506

(Received 5 July 1995)

Environmentally assisted fracture is, in practice, one of the most important fracture modes. We use a large scale atomistic Monte Carlo simulation to study phenomena of the environmentally assisted fracture nucleation in solids with grain boundaries. We study a bicrystal under a tensile stress exposed to an oxidizing atmosphere. We identify conditions under which this environment can significantly enhance intergranular fracture nucleation processes. We find that the nucleation of intergranular microcavities may occur in a region that is well in front of the oxidized zone of the sample, apparently due to inhomogeneous stresses induced by the presence of oxide particles. This effect *increases* with *decreasing* oxidation rate, since then the oxidation front becomes fuzzier and inhomogeneous stresses become stronger. Similar trends were observed in superalloys in which the environmental embrittlement effects are strong for slower oxidation rates, whereas at higher oxidation rates the embrittlement may be suppressed.

I. INTRODUCTION

Fundamental aspects of the fracture physics, such as the very nature of the state of a stressed solid and the role of thermal fluctuations have been addressed in a number of recent studies [1–6]. Stressed solids are metastable states of matter similar to, say, supercooled liquids. In this picture, the failure threshold corresponds to a metastability limit (spinodal point) at which the external stress σ as a function of strain reaches its maximum $\sigma_{\max}$ [4].

If the external tensile stress is smaller than $\sigma_{\max}$, the stressed solid will still break, however, with a *time-delayed fracture*. The sample lifetime depends on the temperature and the applied stress [7]. This phenomenon is believed to be directly related to the processes of *microcavity nucleation* and *growth* [6]. Recent theoretical studies of time-delayed fracture have discussed this phenomenon in monocrystals and in the absence of an environment surrounding the stressed solid [4,5]. However, most of the technologically interesting materials are *polycrystals* and the *intergranular fracture* is in practice one of the most important fracture modes [8]. Moreover, the *environment* plays an important role in assisting fracture nucleation and growth both in mono and in polycrystals [7,8]. An example is the oxygen embrittlement observed in polycrystalline nickel based superalloys [9–11].

In this work we address fundamental physical aspects of environment fractures—their nucleation and growth. Here we present results of the very first atomistic Monte-Carlo simulation of fracture nucleations (time-delayed fractures) in a polycrystal immersed in an oxidizing atmosphere chemically reacting with the stressed solid. We use our simulation to identify conditions under which the environment can significantly enhance fracture nucleation processes. Under some conditions, we find that the nucleation of intergranular microcavities may occur in a region which is well in front of the oxidized zone of the sample, apparently due to inhomogeneous stresses induced by the presence of oxide particles. In-

terestingly enough, this effect *increases* with *decreasing* oxidation rate since then the oxidation front becomes fuzzier and inhomogeneous stresses stronger. Similar trends were observed in superalloys in which the environmental embrittlement effects are strong for smaller oxidation rates, whereas at higher rates the embrittlement may be suppressed.

Layout of this paper is as follows: in Sec. II we describe our Monte-Carlo simulation. The simulation is used to investigate environmental embrittlement effects described in Sec. III. The physical origin of the embrittlement phenomena is clarified in Sec. IV. We use our results to introduce a physical model for the kinetics of the environmentally assisted crack growth discussed in Sec. V. We summarize our results in Sec. VI.

II. MONTE-CARLO SIMULATION

Atomistic (off-lattice) Monte-Carlo (MC) simulations are, at present, a unique modeling method capable of treating extremely slow fracture nucleation phenomena characterizing time-delayed fractures [4–6]. To date, Monte-Carlo dynamics has been used to study fracture nucleation in mono [4–6], and in polycrystals [6], in *vacuum*. Here we incorporate an atmosphere chemically reacting with a solid polycrystalline sample (say, an alloy) under an external tensile stress (see Figs. 1 and 2). In our simulation we have three molecular species, namely, three species of *united atoms* representing the "alloy," "oxygen," and "oxide molecules." We model their interactions by pairwise Lennard-Jones potentials, $U_{\alpha\beta}=4\epsilon_{\alpha\beta}[(\sigma_{\alpha\beta}/r)^{12}-(\sigma_{\alpha\beta}/r)^6]$, where α,β stand for alloy, oxygen or oxide. In addition to the standard atomistic Monte-Carlo dynamics [4–6], here we include a chemical reaction, namely, an *irreversible* oxidation fusing alloy and oxygen molecules into oxide molecules, i.e.,

$$\text{alloy} + \text{oxygen} \rightarrow \text{oxide} . \tag{1}$$

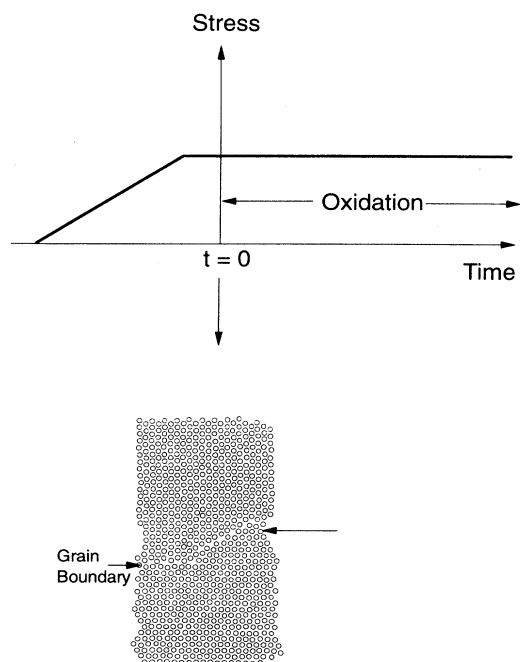Thus, each Monte-Carlo cycle (MCC) of our simulation

FIG. 1. In our simulations we created a sample with a grain boundary. The sample is under a vertical external tensile stress which depends on time as shown in the figure. At some instant of time (time=0) the sample is surrounded by the oxygen atmosphere and oxidation starts.

involves a sequence of standard MC trial atomic moves of all particles followed by a sequence of chemical reaction trial moves. A *trial* chemical reaction move is a fusion of an alloy and oxygen molecule which is done with the probability f_{ox} ("oxidation rate") if the distance between molecules is smaller than a critical distance r_{ox} and zero otherwise. After the reaction, the alloy-oxygen pair is replaced by an oxide molecule. In reality r_{ox} is comparable to the range of interatomic forces. In our simulations we set $r_{ox} = 1.2\sigma_{alloy\text{-}oxygen}$. Irreversible chemical reactions such as (1) release an energy significantly bigger than $k_B T$. Due to this, the standard Metropolis MC algorithm accepts with probability 1 any of the trial chemical reaction moves.

In our simulations we have extensively investigated a two-dimensional solid sample with a single grain boundary, i.e., a bicrystals (Fig. 1). The sample is studied under a vertical tensile stress. The sample was prepared in the absence of the atmosphere (in vacuum) by joining two monocrystals along their crystalline planes. After equilibration initially flat grain boundary becomes rough (see Fig. 1). The sample configuration just before creating the oxidizing atmosphere around it is given in Fig. 1.

III. ENVIRONMENTAL EMBRITTLEMENT EFFECTS

In Fig. 2 we present time evolutions of the stressed sample in three characteristic cases: in vacuum; in case

TABLE I. Lennard-Jones potential parameters used in the simulations.

α-β	$\sigma_{\alpha\beta}$	$\varepsilon_{\alpha\beta}$
alloy-alloy	1	1
alloy-oxide	1	1.5 (rigid oxide) / 0.75 (soft oxide)
oxide-oxide	1	1.5 (rigid oxide) / 0.75 (soft oxide)
oxygen-oxygen	1	0.05
alloy-oxygen	0.57	0.25
oxide-oxygen	0.57	0.25

Vacuum   Rigid oxide   Soft oxide
                rate .001   rate .001

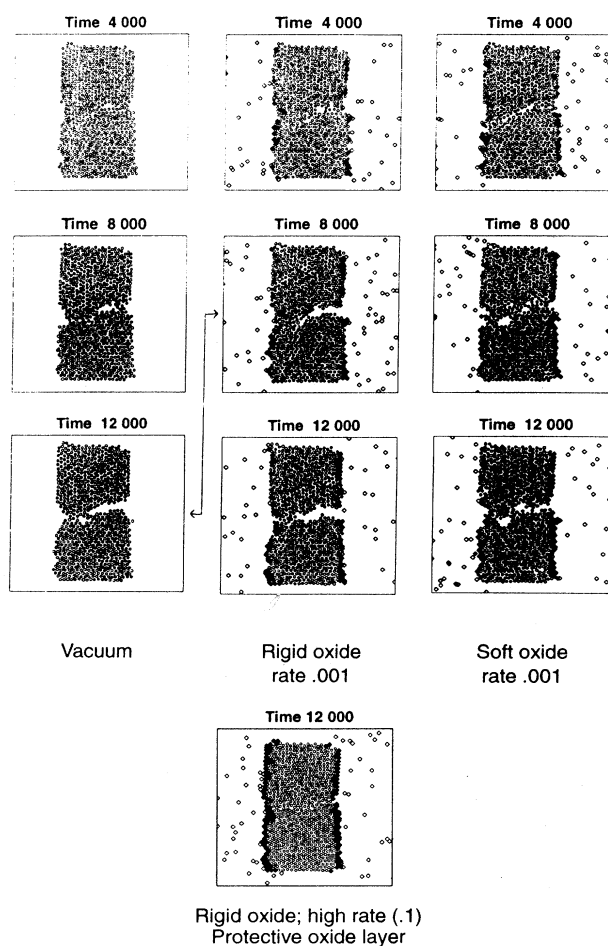Rigid oxide; high rate (.1)
Protective oxide layer

FIG. 2. Evolution of a stressed bicrystal in vacuum; with rigid; and with a soft oxide. The alloy molecules are indicated as circles; oxygen molecules as white squares; and oxide molecules as black squares. Time is measured from the instant when the oxidation started (see Fig. 1). In all the cases the oxidation rate is the same, $f_{ox} = 0.001$, and the applied tensile force is $f = 30$. Note that the rigid oxide assists the intergranular fracture (compare, for example, $t = 12\,000$ MCC in vacuum with $t = 8000$ MCC with a rigid oxide). We present also a sample with the rigid oxide at $t = 12\,000$ MCC, obtained with a higher oxidation rate, $f_{ox} = 0.1$ (see the bottom figure). Then a protective oxide layer is formed and the fracture is suppressed.

of a "rigid" oxide with cohesion energy greater than that of the alloy ($\epsilon_{\text{oxide-oxide}} > \epsilon_{\text{alloy-alloy}}$); and in case of a "soft" oxide with cohesion energy smaller than that of the alloy molecules ($\epsilon_{\text{oxide-oxide}} < \epsilon_{\text{alloy-alloy}}$). The corresponding parameters of the Lennard-Jones (LJ) potential $\epsilon_{\alpha\beta}$ and $\sigma_{\alpha\beta}$ used in our simulations are given in the Table I. Note that LJ core sizes $\sigma_{\alpha\beta}$ are the same for the molecules forming solid phases (alloy and oxide). In this way we exclude internal stresses that may arise due to a difference in molecular sizes between alloy and oxide molecules—they may break the sample even in the absence of externally applied forces [12]. However, here we confine our attention to simpler but still practically interesting situations with no significant difference in molecular sizes so

that the presence of externally applied forces is *still* necessary to fracture the sample. The physical nature of environmental embrittlement phenomena under these conditions is far less known in spite of their practical importance [9–11]. Our results presented in the following may help to understand the nature of these embrittlement phenomena.

Figure 2 documents an embrittlement produced by oxide formation. In all three cases presented in this figure (sample in vacuum; with a rigid oxide; and with a soft oxide) the fracture is time delayed in nature. We see that the situation with *rigid* oxide at time = 8000 MCC is like that in vacuum at a *longer* time = 12 000 MCC. Interestingly enough, it thus appears that the presence of a *rigid* oxide (with a cohesion energy *higher* than the alloy) enhances the rate of intergranular fracture nucleation and growth. We find, however, that this seemingly strange embrittlement occurs only at *small* oxidation rates. With high oxidation rates we find that a protective

Rigid oxide; time 1 000

Rigid oxide; time 2 000

Rigid oxide; time 3 000

Rigid oxide; time 4 000

Rigid oxide; time 5 000

Rigid oxide; time 6 000

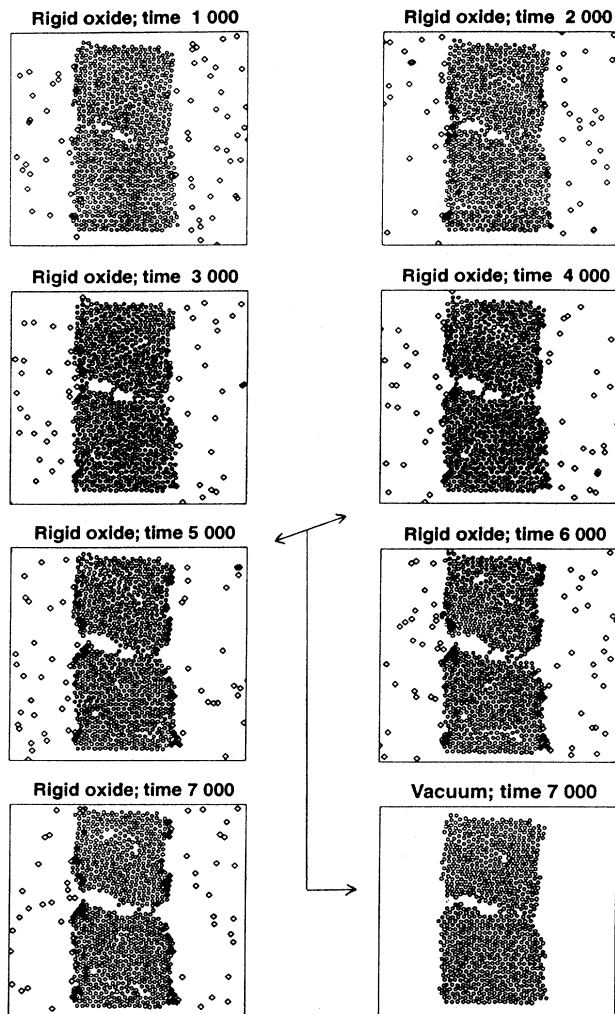**Rigid oxide; time 7 000**

Vacuum; time 7 000

FIG. 3. Evolution of a stressed bicrystal with the rigid oxide formation; here the applied tensile force is $f = 40$. For comparison, we give the sample obtained in vacuum with the same force at time = 7000 MCC. Note that this sample is similar to the oxidized sample at an *earlier* time between 4000 and 5000 MCC.

Vacuum; time 7 000

Rigid oxide; rate .001; time 7 000
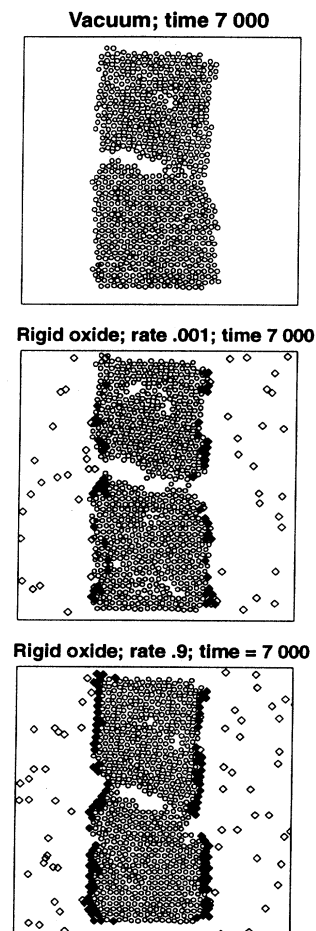
Rigid oxide; rate .9; time = 7 000

FIG. 4. Samples obtained at time = 7000 MCC in vacuum; with small a oxidation rate $f_{\text{ox}} = 0.001$ yielding patches of the oxide; and with a high oxidation rate $f_{\text{ox}} = 0.9$ yielding a continuous oxide layer. In all the cases the applied tensile force is $f = 40$.

oxide layer is formed and the fracture is slowed down (see Fig. 2, bottom). In Fig. 3 we give another example from our simulations now done with a slightly stronger tensile force. Note that the sample in vacuum at time = 7000 MCC is comparable to the oxidized sample (with the rigid oxide) at an *earlier* time between 4000 and 5000 MCC. Once again we see that the presence of the oxide *stimulates* the fracture growth.

An important feature of this environmental fracture enhancement is its dependence on the character of the oxide morphology. In Fig. 4 we compare the sample of the Fig. 3 at time = 7000 MCC (the middle of Fig. 4) with a sample obtained at the same time with a higher oxidation rate (the bottom of Fig. 4), and, also, with a sample obtained in vacuum. Note that, for the high rate, a continuous, apparently "protective" layer is formed on the surface of the sample. On the other hand, for the small rate the oxide is discontinuous—it is formed in *patches*. Note that the *fastest* intergranular fracture growth is observed for the *small* oxidation rate (the middle of Fig. 4) when the oxide is formed in patches rather than a continuous layer. The same *anticorrelation* between the oxidation rate and the fracture extent is evident also in the simulations in Fig. 2 (done at a stress weaker than that in Figs. 3 and 4). There the sample obtained with a high oxidation rate even remained undamaged (see the bottom of Fig. 2) in contrast to the samples obtained with a small oxidation rate.

Similar trends have been observed in stressed nickel-based superalloys in air [9–11]. There, at temperatures around 700 °C one has a slow rate of oxide formation and the strongest embrittlement effects. At higher temperatures there is a fast formation of oxides in the form of a

protective layer and no embrittlement is observed around 1000 °C.

IV. PHYSICAL ORIGIN OF THE EMBRITTLEMENT PHENOMENA

We saw that two conditions favor these environmental fracture nucleation phenomena: (i) a low oxidation rate ensuring that the oxide forms in patches, *not* as a continuous layer (recall Figs. 2–4), and (ii) the oxide has to be *more* rigid than the alloy. These two conditions apparently *conspire* to enhance fracture nucleation and produce time-delayed fractures which are faster than those in polycrystals stressed in vacuum. The physical reason for this is indicted in the Fig. 5: oxide patches are more rigid than the alloy (i.e., they have a bigger elastic modulus than the alloy). Thus, in the nonoxidized alloy regions between the patches one has *local stretching stresses* which *exceed* that in the bulk. These local
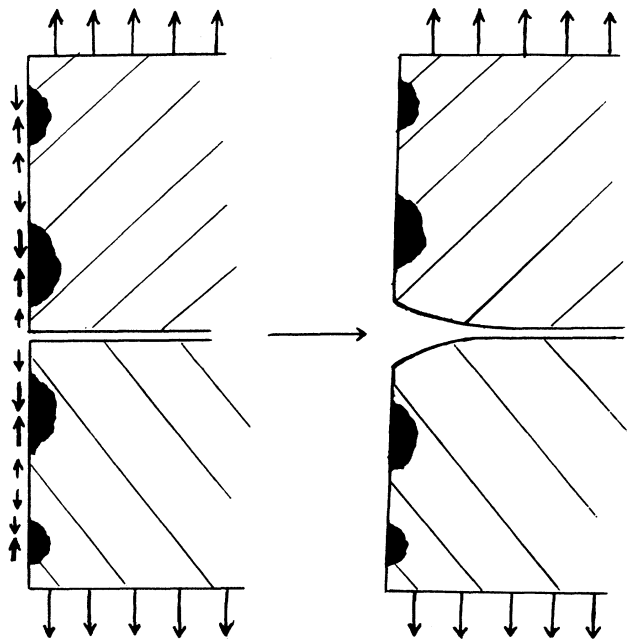

FIG. 5. Rigid oxide patches (black) are causing local stretching stresses which assist in the opening of a grain boundary going between the patches.
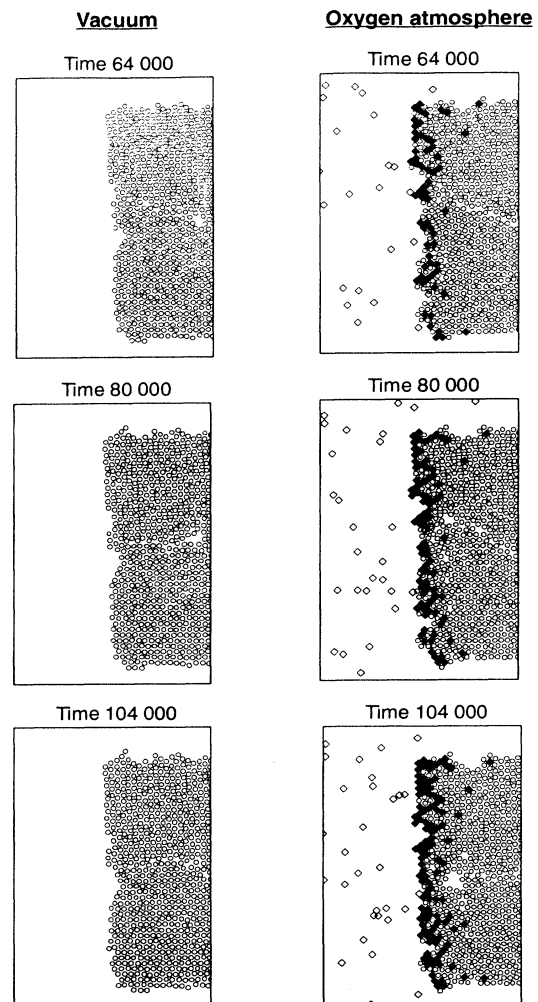

FIG. 6. Oxide patches assist nucleation of an intergranular microcavity. For comparison, we also give the situation for the same sample in vacuum.

stresses may thus assist in the opening of the grain boundary as schematized in Fig. 5. Thus, a rigid oxide formed in patches or, in general, fuzzy oxide fronts, may significantly enhance fracture nucleation in stressed polycrystals. This is illustrated also by another set of our simulations (see Fig. 6), now performed with an applied tensile stress weaker than those in Figs. 2–4. This yields a slower time-delayed fracture and thus enables to resolve details of the kinetics. From these simulations we find that the oxide patches enhance nucleations of *intergranular microcavities*. This is documented in Fig. 6 from our simulations, which illustrates a nucleation of an intergranular microcavity in the presence of the oxide, and the *absence* of such nucleation in a sample exposed to the same external force in vacuum.

This fracture nucleation enhancement is efficient at smaller oxidation rates when the rigid oxide is formed in patches rather than as a continuous layer. The presence of a continuous rigid oxide layer would protect, by its higher cohesion energy, the sample from fracturing (as documented in Fig. 2, bottom, and Fig. 4, bottom). On the other hand, the rigid oxide formed in patches locally increases the stress level in the nonoxidized alloy regions

FIG. 7. Physical picture of the environmentally assisted intergranular crack growth.

between the patches. This assists the intergranular fracture along those grain boundaries which go through the alloy material between the oxide patches, as indicated in Fig. 5 and documented by our simulations in Figs. 2–4.

V. ENVIRONMENTALLY ASSISTED INTERGRANULAR CRACK GROWTH

Based on our observations, we propose here a physical model for environmentally assisted intergranular crack creep growth in polycrystals such as superalloys in air [9,10], see Fig. 7: first, as discussed in Sec. IV, the grain boundary opening is helped by the internal stresses induced by the oxide patches assisting the nucleation of intergranular microcavities [Fig. 7(a)]. Then the oxygen can go further and produce new oxide patches which are now on the walls of the open intergranular microcavities [Fig. 7(b)]. These new oxide patches then assist in opening the new grain boundary portions, and so on. As this process repeats itself [Fig. 7(c)], the crack grows.

This mode of the crack growth will be efficient under conditions found in Sec. IV, namely, if the oxide is more rigid than the alloy, and the oxidation rate is small enough so that the oxide is formed in patches. In practice, the latter condition is violated at higher temperatures since oxidation rates generally grow with increasing temperature and the oxide forms as a protective continuous layer. This implies that, within our model, the rate of the crack growth versus temperature must have a maximum at some characteristic temperature: indeed, starting from low temperatures, initially one must have an increase of the thermally activated creep crack growth rate with increasing temperature. This is, of course, the case both in a vacuum and in an oxygen atmosphere. However, in an oxygen atmosphere the crack growth rate can exceed that in vacuum, if a rigid oxide is formed in patches. Patches produce internal stresses exceeding that in the bulk and thus assist the opening of grain boundaries going between oxide patches, as discussed in Sec. IV. This effect can be, however, *suppressed* by increasing temperature beyond some characteristic temperature. At temperatures higher than that, oxidation is fast and the oxide forms as a continuous protective layer. This suppresses the crack growth by closing entrances to grain boundaries (as in Fig. 2, bottom, and in Fig. 4, bottom)—this mechanically protects grain boundaries (since a rigid oxide has a higher cohesion energy) and, moreover, prevents oxygen to enter grain boundaries and propagate along them. Thus, within our model, the crack growth rate versus temperature must have a maximum at some characteristic temperature above which oxidation rate is high and the oxide forms as a continuous layer. This is evidently the case in nickel-based superalloys in air [9–11]. There one has the highest growth rate of environmental cracks in an intermediate range of temperatures whereas at higher temperatures the environmental fractures growth can be completely suppressed. This experimental phenomenology is thus in agreement with our model.
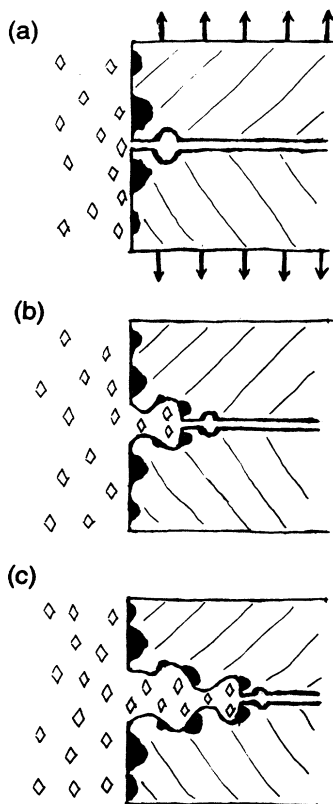
VI. SUMMARY

To summarize, we developed the atomistic Monte-Carlo simulation of environmental assisted fractures in polycrystalline solids chemically reacting with an oxidizing atmosphere. Our results document enhanced fracture nucleation related to the mechanical effects of oxides. Generally, rigid oxides can produce a significant enhancement of the fracture nucleation and growth. This enhancement is, however, sensitive to the oxidation rate determining the morphology of the oxide front. Thus, smaller rates, ensuring formation of the oxide in patches, quite effectively assist the fracture nucleation. On the other hand, higher rates produce continuous oxide layers which mechanically protect the sample and slow down the failure. Finally, we used our results to arrive, in Sec. V, at a physical model for the environmentally assisted intergranular crack growth. Variations of the crack growth rate with temperature observed in superalloys can be rationalized within our model.

ACKNOWLEDGMENTS

[1] K. Nishioka and J. K. Lee, Philos Mag. A **44**, 779 (1981).

[2] R. L. B. Selinger, Z.-G. Wang, W. M. Gelbart, and A. Ben-Shaul, Phys. Rev. A **43**, 4396 (1991).

[3] Z.-G. Wang, U. Landman, R. L. B. Selinger, and W. M. Gelbart, Phys. Rev. B **44**, 378 (1991).

[4] R. L. B. Selinger, Z.-G. Wang, and W. M. Gelbart, J. Chem. Phys. **95**, 9128 (1991).

[5] L. Golubović and S. Feng, Phys. Rev. A **43**, 5223 (1991).

[6] L. Golubović and A. Peredera, Phys. Rev. E **51**, 2799 (1995).

[7] S. S. Brenner, in *Fiber Composite Materials* (American Society for Metals, Metals Park, OH, 1965), p. 11.

[8] S. F. Pugh, *An Introduction to Grain Boundary Fracture in Metals* (The Institute for Metals, London, 1991).

[9] C. A. Hippsley and J. H. DeVan, Acta Metall. **37**, 1485 (1989).

[10] P. Valerio, M. Gao, and R. P. Wei, Scr. Metall. Mater. **30**, 1269 (1994).

[11] Bruce Kang (private communication).

[12] H. J. Grabke, M. Steinnhorst, M. Brumm, and D. Weiner, Oxid. Met. **35**, 199 (1991).